Article

Assessment of Long-Term Thermal Aging Effects on PVC/Al$_2$O$_3$ Nanocomposites Through Electrical, SEM and FTIR Characterizations

Sabrina Amraoui [1], Abdallah Hedir [1,2,*], Mustapha Moudoud [1], Ali Durmus [3], Sébastien Rondot [4], Abderrahmane Manu Haddad [2,*] and David Clark [2]

[1] Laboratoire de Technologies Avancées en Génie Electrique, Université Mouloud Mammeri de Tizi Ouzou, Tizi-Ouzou BP 17 RP, Algeria; sabrina.amraoui@ummto.dz (S.A.); mustapha.moudoud@ummto.dz (M.M.)

[2] Advanced High Voltage Engineering Centre, School of Engineering, Cardiff University, Queen's Buildings, The Parade, Cardiff CF24 3AA, UK; clarkd@cardiff.ac.uk

[3] Department of Chemical Engineering, Engineering Faculty, Istanbul University-Cerrahpaşa, Istanbul 34320, Turkey; durmus@iuc.edu.tr

[4] Laboratoire Matériaux et Ingénierie Mécanique, UFR Sciences, Université de Reims Champagne Ardenne, BP1039, 51687 Reims, France; sebastien.rondot@univ-reims.fr

[*] Correspondence: abdallah.hedir@ummto.dz (A.H.); haddad@cardiff.ac.uk (A.M.H.)

Abstract

This study investigated the effect of nanofiller on the structural properties of thermally aged polyvinyl chloride (PVC)/Aluminum oxide (Al$_2$O$_3$) nanocomposites prepared with different amounts of nanoparticles (2.5, 5.0, and 7.5 wt%) using various techniques. Experimental studies were designed to monitor structural changes in PVC/Al$_2$O$_3$ nanocomposites by means of dielectric characterization, charging and discharging currents measurements, SEM and FTIR analyses, and visual observations as a function of nanofiller amount and aging time. The results obtained demonstrated that the dielectric permittivity of PVC was increased for unaged samples with the addition of 2.5% and 7.5% Al$_2$O$_3$ nanoparticles. An increase in dielectric losses is also observed at the same level of filler content, attributable to interfacial polarization driven by improved charge transport and dipole relaxation. A decrease in charging and discharging currents with higher Al$_2$O$_3$ content is attributed to an increase in matrix rigidity, which restricts charge carrier mobility. The charging and discharging currents progressively increased during thermal aging, as polar aging products were formed during this process, which could improve charge mobility and conductivity. FTIR and SEM analyses indicated that with thermal aging, polar groups formation was more likely due to structural decomposition of the matrix and mild dehydrochlorination. The changes in color were indicative of surface degradation. These results provide new insight into the electrical and aging behaviors in PVC/Al$_2$O$_3$ nanocomposites.

Keywords: polyvinyl chloride (PVC)/aluminum oxide (Al$_2$O$_3$); nanoparticles; dielectric characterization; SEM; FTIR

1. Introduction

Polymer nanocomposites are increasingly investigated for their potential use in industry, especially in energy applications [1]. There is growing research interest in polymer nanocomposites [2] due to their outstanding electrical [3], mechanical, optical, and thermal performances [4,5].

Polyvinyl chloride (PVC) has been widely used as a dielectric material in power cables because of its distinctive properties, including low cost, low dielectric constant, ease of fabrication, and high dielectric strength [6]. Despite the advantageous characteristics, PVC lacks stability when exposed to service conditions such as mechanical, electrical and thermal stresses, and chemical aging. To mitigate these shortcomings, various additives, particularly nanofillers, have been investigated in PVC formulations at the research level to improve performance [7]. According to the literature, it is well established that the introduction of nanofillers into the PVC matrix improves its properties [8]. Sugumaran [9] reported that SiO_2 and $CaCO_3$ enhance the mechanical and electrical properties of PVC. Nait Larbi et al. [10] demonstrated that the addition of $CaCO_3$ into the PVC matrix can improve the dielectric properties of the base PVC. Yaacob et al. [11] stated that the reinforcement of PVC with wollastonite ($CaSiO_3$) improves its dielectric characteristics. Faiza et al. [12] showed that adding ZnO particles improves the hydrophobic properties of the base PVC. Xie et al. [13] showed that PVC/ZnO provides enhanced stability under environmental stress.

High operating temperatures can affect the properties of PVC nanocomposites over time. Therefore, it is essential to conduct long-term testing of these nanocomposite materials before their deployment into practical applications. Several research works have focused on studying unfilled polymer materials under thermal aging [14,15] but research on the effects of temperature on PVC nanocomposites, especially PVC/Al_2O_3, is scarce and the underlying mechanisms of deterioration are still unclear.

Al_2O_3 is favored in many applications because it combines high thermal conductivity, great chemical stability, and excellent electrical insulation [16]. When Al_2O_3 is incorporated into polymer matrices, it has been shown to lower ignition susceptibility and to decrease the rate of heat release during thermal decomposition [17]. Maur et al. [18] concluded that the addition of Al_2O_3 nanoparticles significantly reduces trapped charge formation and reduces the thermal degradation of epoxy resin. This makes Al_2O_3 especially well-suited for applications that demand long-term thermal and dielectric stability, such as cable insulation.

In this work, the effects of long-term thermal aging on the properties of a PVC/Al_2O_3 nanocomposite have been investigated. The preparation of PVC/Al_2O_3 nanocomposites is carried out considering different nanofiller amounts of Al_2O_3. These filler loadings are 0, 2.5, 5, and 7.5 wt%. Electrical behavior is investigated by measurements of dielectric constant, loss factor and loss index, and of the charging–discharging current before and after thermal aging. The chemical structure of PVC/Al_2O_3 nanocomposites is investigated using Fourier Transform Infrared (FTIR) spectroscopy. The change in surface morphology is evaluated with Scanning Electron Microscopy (SEM) analysis.

The key findings of this study are as follows:

- Al_2O_3 nanoparticle addition significantly enhances the thermal aging resistance of PVC.
- Dielectric permittivity and the dielectric loss factor are better maintained in nanocomposites than in pure PVC, indicating improved dielectric stability.
- Charging and discharging currents decrease with increasing Al_2O_3 content, demonstrating an improvement in the insulation performance.
- Charging and discharging currents increase over time. These increases are attributed to the formation of aging products and reactive molecular groups, which enhance charge carrier mobility, and consequently raise the conductivity of PVC.
- FTIR and SEM analyses revealed that thermal aging led to the development of certain polar groups, likely because of structural breakdown and slight dehydrochlorination. Additionally, a distinct color change was observed in the samples over the course of aging, suggesting surface degradation.

2. Experimental Setup

The samples investigated in this study were prepared at the ENICAB laboratory (Entreprise Nationale de l'Industrie du Câble, Biskra, Algeria) using a commercial PVC resin (grade 4000 M) specifically formulated for wire and cable insulation. This thermoplastic polymer, produced by suspension polymerization, was manufactured by the National Petrochemical Industries Company (ENIP, Skikda, Algeria). The PVC 4000 M matrix was then used to prepare composites with aluminum oxide (Al_2O_3, Sigma-Aldrich, reference 414069-1KG, Pcode: 1002979207, St. Louis, MO, USA) selected as a filler due to its high purity (~99%) and reliable quality. The material was supplied in a porous, pelleted form (~3 mm) and was unmodified, with hydrophilic surface chemistry. The pellets are composed of primary γ-Al_2O_3 particles with a nominal size of <50 nm, a specific surface area of about 31.1 m^2/g, and a spherical morphology. High-shear conditions during calendering were critical for de-agglomerating these pellets and achieving a uniform dispersion of the nanofillers within the PVC matrix, thereby forming a nanocomposite. The Al_2O_3 nanofiller was used without any surface treatment. This was a deliberate choice to study the intrinsic effects of the nanofiller's physical presence and its native interface with the PVC matrix on the aging behavior.

The PVC/Al_2O_3 nanocomposites were prepared by introducing different filler proportions of 2.5, 5.0, and 7.5 wt% into a PVC matrix. The PVC/Al_2O_3 composite samples were fabricated using a Polymix 200 P calendering system (Brabender, Duisburg, Germany), which features two independently controlled heated rollers. For this process, the roller temperatures were maintained at 170 °C to ensure proper softening of the polymer blend. A mixture of PVC and Al_2O_3, prepared in specified proportions, was applied directly to the pre-heated rollers. The mixing and lamination process was conducted at a temperature of 165 °C for approximately 15 min. Final specimens had dimensions of 50 mm × 50 mm with a thickness of 1.5 mm. The selected filler contents of 2.5%, 5%, and 7.5% were based on findings from the previous literature, showing that nanofiller loadings in the 1–5 wt% range enhanced dielectric and thermal properties without causing agglomeration [19,20]. The 7.5% level was included to investigate the upper limit of effective dispersion and its impact on aging behavior.

In this study, a continuous isothermal heating protocol was conducted using a thermo-ventilated oven fixed at a constant temperature of 90 ± 2 °C. The samples were placed vertically and heated in the oven for 2400 h. The aging temperature was selected to hasten thermal degradation while remaining near practical service levels, since cable insulations normally function at 70–85 °C. This modestly elevated temperature promotes aging processes to evolve in a manageable duration yet avoids initiating degradation mechanisms that would not occur under normal operating conditions. Measurements of charging/discharging currents, and FTIR and SEM analyses were conducted at 0, 1200, and 2400 h. Dielectric measurements were performed after each 240 h of aging.

An LCR meter (Instek-LCR 817 type, Good Will Instrument Co., Ltd., New Taipei city, Taiwan) was used to characterize the studied material. The LCR meter was set up to measure the capacitance and dielectric loss factor ($\tan\delta$) of the samples at a frequency range of 10^1–10^4 Hz. We studied dielectric behavior across this frequency range as it provides a highly sensitive window to characterize the fundamental material properties and interfacial polarization phenomena induced by the nanofillers. At this frequency, the contributions of interfacial polarization at the polymer–nanoparticle boundaries are pronounced, allowing for a clearer distinction between the different composite formulations and their aging states. The dielectric constant (ε') and dielectric loss index (ε'') were calculated by using Equations (1) and (2):

$$\varepsilon' = \frac{d}{A \cdot \varepsilon_0} \cdot C \tag{1}$$

$$\varepsilon'' = \tan\delta \cdot \varepsilon' \tag{2}$$

where d, A, C, and ε_0 are the sample thickness, area of sample in contact with the electrode, capacitance of the sample, and the permittivity of the free space (8.85×10^{-12} F/m), respectively.

The charging and discharging currents were measured using an automated Hewlett-Packard 4140B picoammeter/voltage source (Keysight Technologies, Palo Alto, CA, USA). The charging current was measured by applying 100 V dc for 100 s. After the applied voltage was removed and the sample was short-circuited through the electrometer, the discharging current was measured for the same period. The current measurements were carried out under ambient conditions.

To ensure statistical reliability, all dielectric and current measurements were performed in two separate campaigns. The LCR meter had a stated precision of 0.05%, and the picoammeter had a specified accuracy of $\pm$(0.4% of the reading + 2 fA), ensuring high-fidelity data acquisition.

SEM analyses were carried out with the JEOL Microscope model 6460LV (JEOL Ltd., Akishima, Japan). The images were obtained using the secondary electron detector, under an acceleration voltage of 20 kV, a reduced probe size, and a working distance of 9 mm. To limit the effects of charges by electron bombardment of the PVC surface, the samples were cleaned in an ultrasonic tank and a 15 nm thick Gold/Palladium alloy layer (Ted Pella, Inc., Redding, CA, USA) deposited on their surface by vacuum evaporation.

FTIR characterization was performed using a Shimadzu-8400S type spectrometer (Shimadzu Corporation, Nakagyo-ku, Kyoto, Japan). Unaged and aged samples were scanned in the spectral range 650–4000 cm^{-1} with a resolution of 4 cm^{-1}. A total of 50 scans were carried out for each sample.

Photographs of both unaged and thermally aged specimens were captured using a camera and subsequently compared to assess the extent of color variation.

3. Results and Discussion

3.1. Dielectric Characterization

Figure 1 shows the measured dielectric constant, dielectric loss factor, and dielectric loss index at 10 kHz as a function of filler content before thermal aging.
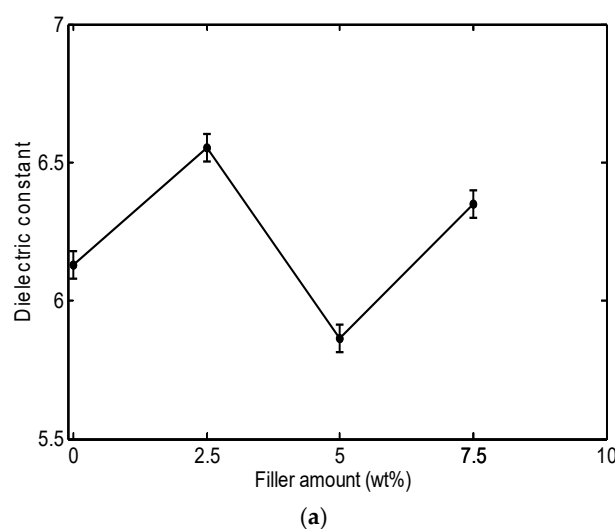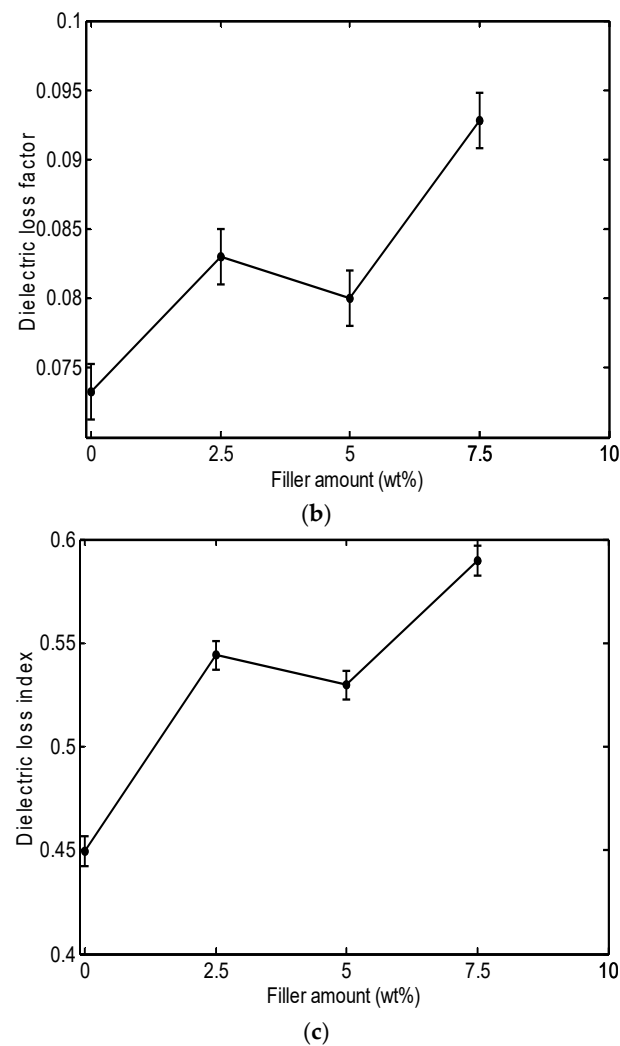

(a)

Figure 1. *Cont.*

Figure 1. Dielectric properties of PVC/Al$_2$O$_3$ nanocomposites as a function of filler content at 10 kHz before thermal aging: (**a**) dielectric constant, (**b**) dielectric loss factor, and (**c**) dielectric loss index.

As shown in Figure 1a, the addition of Al$_2$O$_3$ has a non-monotonic effect on the dielectric constant of PVC, with permittivity increasing by 6.9% at 2.5 wt% and 3.6% at 7.5 wt% loadings. This effect depends on the permittivity of the filler and the restriction of molecular movements in the interaction zone of the nanoparticles. This phenomenon was reported by Mansour et al. [21] when studying the dielectric properties of PVC/ZnO nanocomposites. In general, the dielectric permittivity of PVC nanocomposites depends on the permittivity of the filler as well as the extent of nanoparticle agglomeration [22]. Thus, the interaction between the filler and the polymer matrix, including the dispersion quality of the nanoparticles, plays a significant role in determining the overall dielectric properties. Agglomeration of nanoparticles can lead to inhomogeneous distribution, which can reduce filler effectiveness and affect the dielectric behavior of the composite material. The PVC/Al$_2$O$_3$ composite shows a higher dielectric constant for the amounts of 2.5 and 7.5%, which can be attributed to the dipoles introduced by the nano-structuring. Indeed, at these filler amounts, the polarization increases due to the formation of dipoles by free charges at the polymer–nanofiller interface, as well as the restructuring of polymer chains within the resulting nanocomposite [22]. The 5 wt% Al$_2$O$_3$ sample had a lower dielectric constant than for 2.5% and 7.5%. This observation can be attributed to the better dispersion of the particles, which increases the range of polymer–filler interfaces. These interfacial areas fix the motion of the polymer chains, thereby decreasing polarization in

the material. The corresponding SEM images support this as there was a smaller number of large agglomerates in the 5 wt% cases than in the 7.5% cases and these appeared more homogeneous based on visual observation. There was also a reduced spread of the dielectric measurements of the 5 wt% sample, which indicates more stable dispersion. The dispersion in the 5 wt% sample is an intermediate state. The absence of larger agglomerates and the overall improved dispersion decreased dipolar polarization and provided a dielectric response distinct from the 2.5% and 7.5% loading [23]. The reduction in the permittivity value can be explained by the agglomeration of nanoparticles and may additionally have an effect by developing uneven regions in the network which may also decrease effective polarization, thus reducing ε' at this concentration [24].

From Figure 1b, it can be seen that adding Al_2O_3 to the PVC matrix increases the dielectric loss factor, with permittivity increasing by 13% at 2.5 wt% and 26% at 7.5 wt% loadings. This increase is attributed to the morphology of the obtained nanocomposites. Thus, it is important to note that Al_2O_3 can easily adhere to the PVC surface, which in turn leads to increased surface roughness and inhomogeneity [25]. These surface irregularities create areas where charges can accumulate and move more easily, promoting the dissipation of energy in the form of heat, which increases the dielectric loss factor. Furthermore, these defects can also facilitate the passage of electric currents, leading to an increase in the conductivity of the material.

Figure 1c indicates that the dielectric loss index shows practically the same variations as the dielectric loss factor. The heat dissipated in the polymer can be determined by observing the changes in the dielectric loss index. Thus, any increase or decrease in the dielectric loss index directly corresponds to the amount of power dissipated in the material [26]. The increase in the dielectric loss index with increasing filler content can be explained by the increase in local conductivity and the modification of the polymer structure, which leads to increased thermal energy dissipation [27].

Figure 2a illustrates the impact of aging time on the dielectric constant of PVC/Al_2O_3 nanocomposite materials with varying concentrations of Al_2O_3 nanoparticles. This figure indicates that the dielectric constant for both the pure sample and nanocomposite with 5% filler amount remains constant with aging time. The slight decrease in dielectric constant at the end of the aging of PVC with 2.5% and 7.5% Al_2O_3 is attributed to a combination of nanoparticle agglomeration, PVC stiffening, interface changes, internal defect formation, and nanoparticle rearrangement within the polymer [23,28]. These combined factors limit the polarization capability of the material, thus reducing the dielectric constant.

The effect of aging time on the dielectric loss factor for the PVC/Al_2O_3 nanocomposite with various amounts of Al_2O_3 NPs is shown in Figure 2b. It can be observed that the variation in dielectric loss factor of pure PVC, PVC with 2.5% and 5% Al_2O_3 is insignificant. The decrease in the dielectric loss factor of PVC with 7.5% Al_2O_3 with thermal aging is mainly related to improved material organization and reduced charge mobility. The enhancement in the PVC nanocomposite performance leads to reduced energy dissipation in the material, since a lower dielectric loss indicates higher energy storage efficiency and lower heat generation [29].

The evolution of both the dielectric constant and dielectric loss factor over time affects the long-term performance of PVC/Al_2O_3 nanocomposite insulation. A consistent dielectric constant ensures stable insulating performance, whereas an increase may indicate material degradation. The decrease in dielectric loss factor, especially in nanocomposites with 7.5 wt% Al_2O_3, indicates better interfacial stability and lower energy loss, which is advantageous for reducing heat generation when operating in service conditions.
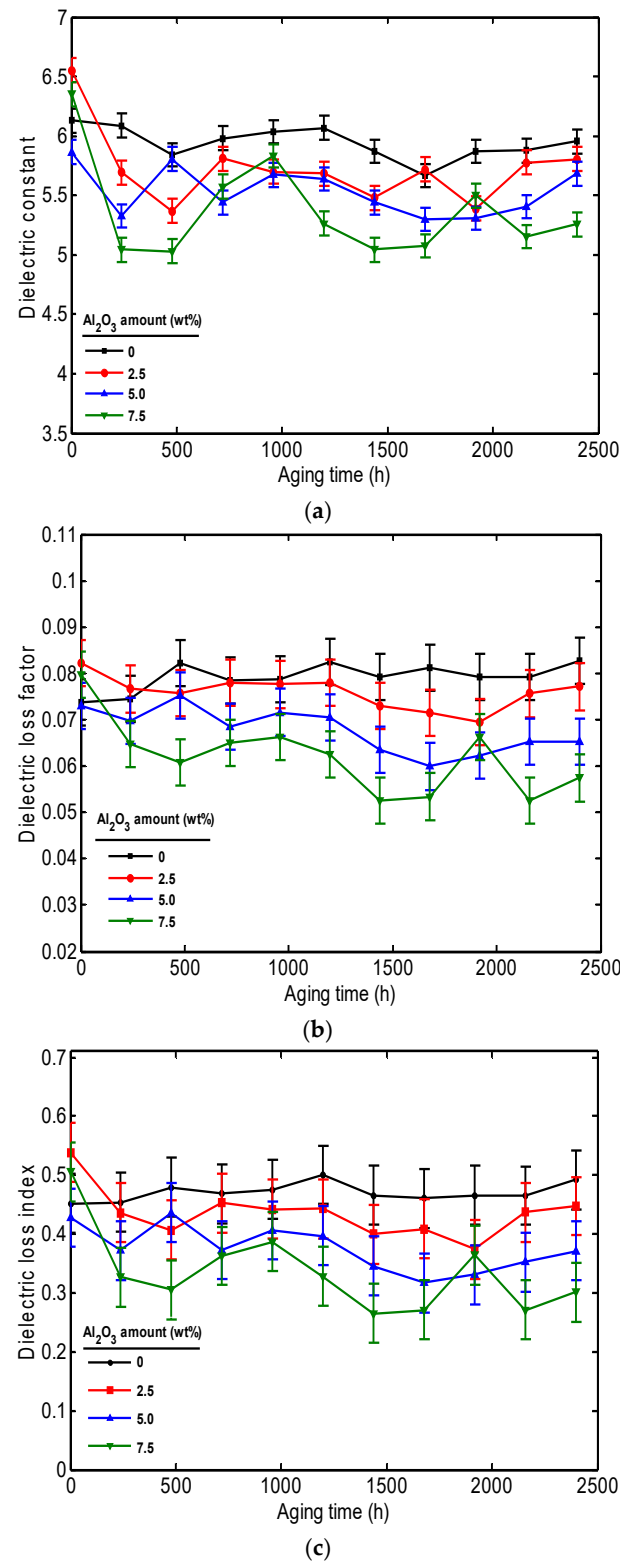
(a)

(b)

(c)

Figure 2. Dielectric properties of PVC/Al$_2$O$_3$ nanocomposites as a function of aging time at 10 kHz: (**a**) dielectric constant, (**b**) dielectric loss factor, and (**c**) dielectric loss index.

Figure 2c displays the evolution of the dielectric loss index with thermal aging time. The variation in this property exactly follows that of the dielectric loss factor, since dielectric loss index is the product of the relative dielectric loss factor and the dielectric constant [30]. The change in this property provides insight into the power dissipated in the

polymer. Consequently, any increase or decrease in the dielectric loss index directly reflects a corresponding rise or fall in the power loss within the material.

3.2. Charging and Discharging Current Measurements

The charging and discharging currents as a function of thermal aging time and filler content are shown in Figure 3. As can be seen in Figure 3a, the charging and discharging currents decreased with more Al_2O_3 fillers, likely due to a more rigid polymer matrix. Indeed, at a steady state the charging current of the pure PVC is 1.74×10^{-11} A, decreasing to 1.41×10^{-11} A for PVC with 2.5% Al_2O_3, 1.33×10^{-11} A with 5% Al_2O_3, and finally 1.25×10^{-11} A with 7.5% Al_2O_3. This result is in accordance with the dielectric changes discussed previously (Figure 1b). The reduction in charging current as the filler content increases can be the result of energy dissipation as heat, often associated with a higher dielectric loss factor, which leads to greater efficiency in energy transfer through the material [31]. The charging current with different filler contents increases with increasing thermal aging time, for example, for the PVC with 7.5% Al_2O_3, the charging current of the unaged sample is 1.25×10^{-11} A, increasing to 1.54×10^{-11} A after 1200 h (Figure 3b), and reaching 1.7×10^{-11} A after 2400 h thermal aging (Figure 3c). The increase in charge currents, often associated with increasing conductivity, is attributed to the degradation of the materials under thermal aging leading to the modification of interfaces, formation of micro-cracks, production of more polar groups, and improvement of charge mobility [32].
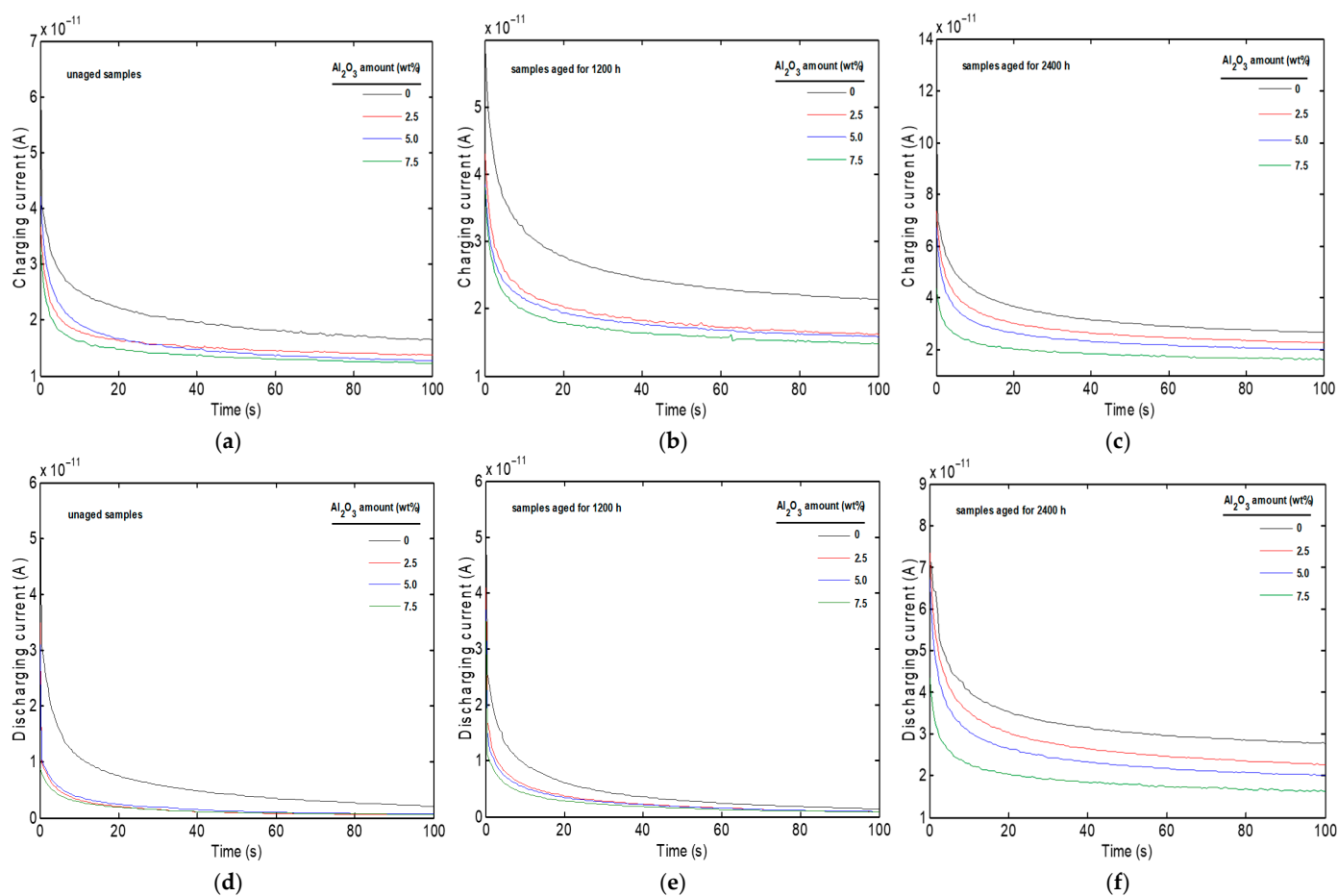

Figure 3. Charging and discharging currents versus time for PVC/Al_2O_3 nanocomposites at different stages of thermal aging: (**a**) Charging currents for unaged samples; (**b**) Charging currents after 1200 h of aging; (**c**) Charging currents after 2400 h of aging; (**d**) Discharging currents for unaged samples; (**e**) Discharging currents after 1200 h of aging; (**f**) Discharging currents after 2400 h of aging.

As can be seen in Figure 3d, the discharging current of the unaged PVC decreases with increasing filler content. At a steady state, the discharging current of the pure PVC is 2.52×10^{-12} A, decreasing to 7.73×10^{-13} A for the PVC with 2.5% Al_2O_3, 6.81×10^{-13} A with 5% Al_2O_3, and finally 5.82×10^{-13} A with 7.5% Al_2O_3. The decrease in discharge currents with increasing Al_2O_3 content is due to charge trapping, increasing the rigidity of the polymer matrix, and modifications in the conductive pathways. At the same time, the discharging current increases with increasing thermal aging time. Taking PVC with 7.5% Al_2O_3 as an example, the discharging current of the unaged sample is 5.82×10^{-13} A, increasing to 1.01×10^{-12} A after 1200 h (Figure 3e), and to 1.66×10^{-11} A after 2400 h thermal aging (Figure 3f). That is explained by thermal aging of polymers, which leads to the formation of aging products, charged particles, and reactive molecular groups. These changes accelerate the discharge process, increase the mobility of charge carriers, and consequently raise the conductivity of these materials, leading to a higher depolarization current [33].

The kinetics of charging and discharging currents can also be interpreted in terms of space-charge dynamics and trap-controlled transport. In the unaged state, the presence of Al_2O_3 introduces interfacial regions that act as additional traps, restricting the motion of charge carriers and lowering the overall current. With thermal aging, chemical and structural modifications such as chain scission, voids, and altered filler–matrix contacts create new trap states and shift their energy distribution. A higher proportion of shallow traps accelerates carrier release and contributes to the observed rise in discharge currents, while deeper traps are responsible for the long-time relaxation tail. These results suggest that the order-of-magnitude increasing in currents after 2400 h is consistent with a combination of space-charge accumulation and trap evolution in the PVC matrix.

3.3. SEM Analysis

SEM images of unaged and aged PVC/Al_2O_3 nanocomposites samples are given in Figure 4. The effect of Al_2O_3 nanoparticle concentration on the microstructural features of specimens can also be particularly observed in this figure.

The specimens loaded with 0, 2.5, and 5.0 wt% Al_2O_3 exhibit similar microstructures and uniform particle dispersion. Large filler agglomerates are clearly seen in the samples loaded with 5.0 and 7.5 wt% Al_2O_3. It is observed that the filler particles become more visible with increasing aging time. The same observation is made for the case of the unloaded PVC, because this sample includes a small number of inorganic additives like stabilizers and processing aids, etc., but is most pronounced for the specimens with Al_2O_3 at loadings of 2.5 and 5.0 wt%. Another remarkable change in the samples is the formation of micro-cracks and voids in the polymer phase with the increase in aging time. The analysis concludes that thermal aging primarily degrades the PVC matrix, manifesting as significant microstructural defects. It can be assumed that the aging temperature (90 ± 2 °C) is not sufficient to trigger the structural degradation of PVC, which is typically initiated by a dehydrochlorination reaction. This is consistent with established polymer chemistry. Observations from the SEM analysis could be attributed to destructive thermal effects impacting the chain dynamics of PVC and probably by causing shrinkage and the formation of voids in bulk structures as well as at polymer–filler interfaces. In addition, a small amount of structural decomposition in PVC chains may have occurred [34]. These physical changes or defects align closely with the observed increases in both charging and discharging currents after 1200 and 2400 h, which implies enhanced mobility of charge carriers likely due to degradation at the filler–matrix interface and the formation of conductive paths through defects [35–37]. In parallel, the reductions seen in the dielectric constant and variations in the loss factor most evident in the 2.5% and 7.5% filler composites can be

linked to disrupted polarization mechanisms and structural heterogeneity caused by filler agglomeration and internal voids. FTIR analysis further supports these findings, with a rise in the I_{1600}/I_{1072} peak ratio signaling progressive chemical changes such as the formation of unsaturated bonds through partial dehydrochlorination. Altogether, these structural and chemical degradations visibly affect the dielectric stability and insulation capacity of the PVC/Al$_2$O$_3$ nanocomposites over time. It can be concluded that thermal aging leads to microstructural defects in the samples and such a destructive effect occurs primarily in the PVC phase.

Aging Time (h)	Al₂O₃ nanoparticles (wt%)			
	0	**2.5**	**5.0**	**7.5**
0 h				
1200 h				
2400 h				
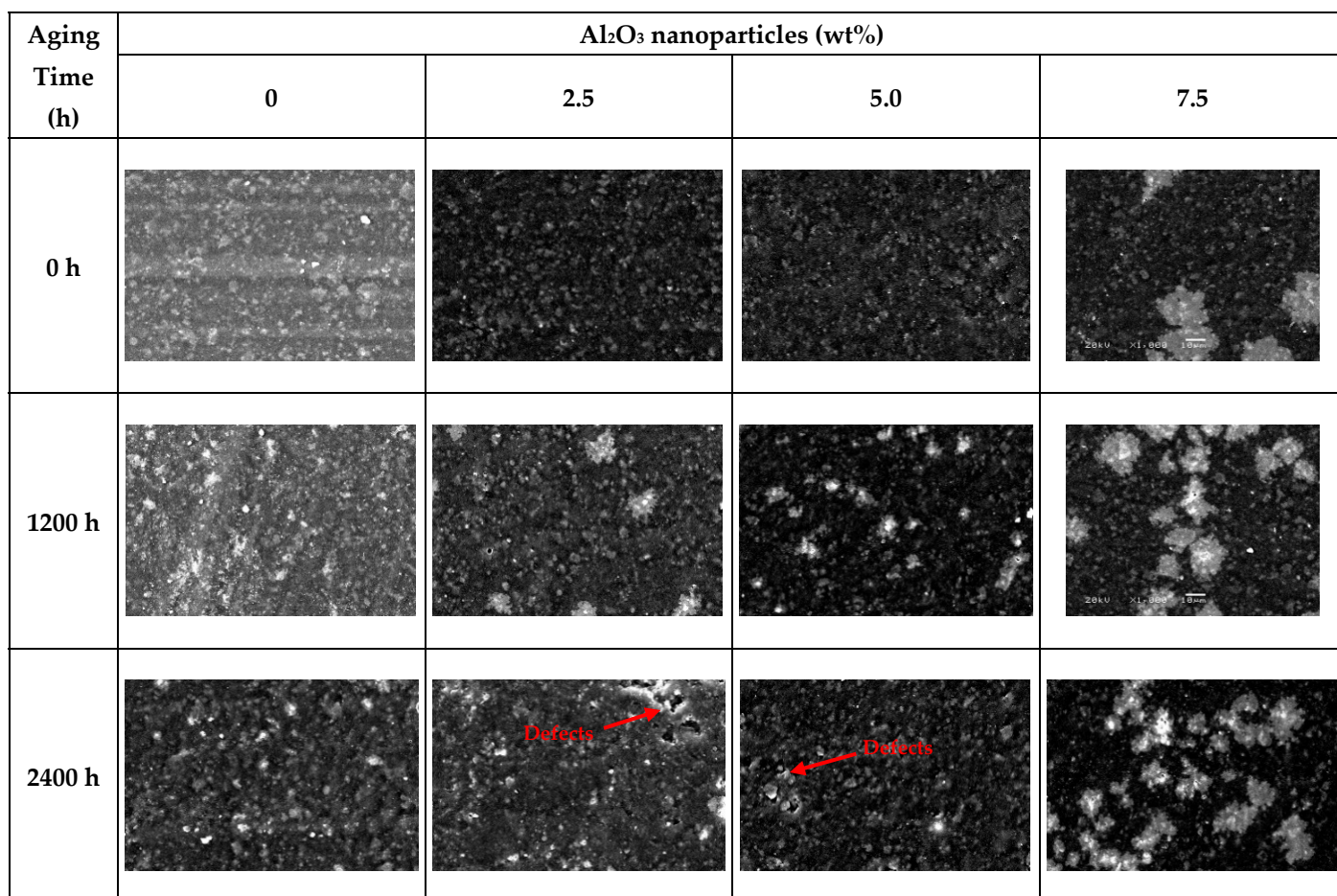
Figure 4. SEM images of virgin and aged samples. Images were taken at 1000× magnification with a scale bar of 10 μm.

3.4. FTIR Analysis

FTIR spectra of unaged samples loaded with different Al$_2$O$_3$ amounts are given in Figure 5a. Characteristic peaks corresponding to functional groups in PVC, plasticizers, and organic additives are seen in the spectra.
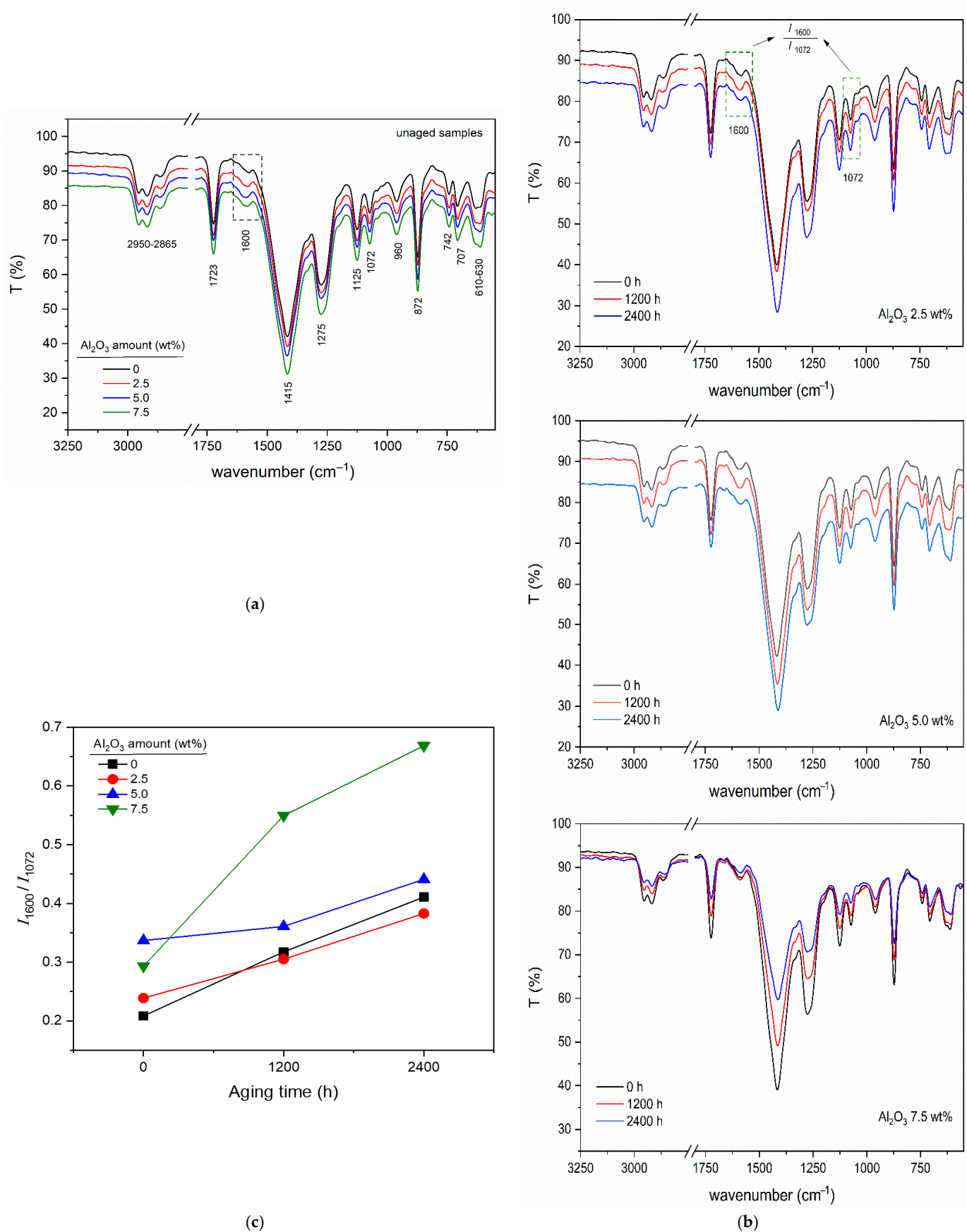
Figure 5. FTIR analysis of PVC/Al$_2$O$_3$ nanocomposites: (**a**) spectra of unaged samples at various filler concentrations, (**b**) spectral evolution with thermal aging time, and (**c**) quantitative analysis of dehydrochlorination via the I$_{1600}$/I$_{1072}$ peak ratio.

The peaks seen in the wavenumber range of 2950 to 2865 cm^{-1} belong to the symmetric and asymmetric stretching of the (C-H) bonds. The specific peaks at 1725 cm^{-1} and 960 cm^{-1} correspond to the stretching vibration of (C=O) and out-of-plane bending vibration of (OH) of stearic acid, used as a processing aid, and of the Ca-St stearate used as a stabilizer in PVC formulations. The peaks seen at 1072 cm^{-1} and 1125 cm^{-1} belong to the stretching vibration of the (C-C) bond and the out-of-plane bending vibration of the (C-H) bond, respectively. The peaks observed at 610–630 cm^{-1} correspond to vibration of the C-Cl bond. The peak at 1600 cm^{-1} indicates the double bond –CH=CH– formed by the dehydrochlorination of PVC. This peak can be used as the decisive signal to quantify the level of structural decomposition depending on the amount of Al_2O_3 nanoparticles and aging time. A reference peak must also be defined to quantify structural changes in PVC chains. In this study, the C-C peak at 1072 cm^{-1} was taken as the reference peak and peak intensity ratios (I_{1600}/I_{1072}) were determined as a function of Al_2O_3 amount and aging time.

Figure 5b shows the FTIR spectra of PVC/Al_2O_3 nanocomposites. Figure 5c illustrates the peak intensity ratios (I_{1600}/I_{1072}) of samples for the mentioned quantification. A higher intensity ratio corresponds to an increase in the number of C=C bonds due to structural degradation. This structural degradation correlates with electrical changes, such as increased charging and discharging currents over time. The observed increase in charging and discharging currents during thermal aging is attributed to a combination of chemical and physical degradation mechanisms. Indeed, the progressive rise in conductivity, evidenced by the increasing charging and discharging currents, points to the co-occurrence of chemical and physical aging mechanisms in thermally aged PVC [38]. Spectroscopic analysis confirms the gradual formation of conjugated polyene structures within the polymer matrix, indicated by the intensifying FTIR absorption at 1600 cm^{-1}, a well-established marker for dehydrochlorination [39]. These chemically transformed regions can facilitate charge transport through electron delocalization along the polymer backbone, effectively creating conductive pathways [40]. In parallel, microstructural analysis reveals the emergence of voids and micro-cracks that create physical pathways for charge migration and injection. The synchronous evolution of the conductive properties with the specific chemical signature of dehydrochlorination, however, indicates that this molecular-level transformation plays a particularly critical role in the initial and pronounced decline of the material's insulating properties during thermal aging [32]. However, in the specific case of PVC, thermal aging and related structural decomposition via dehydrochlorination lead to the formation of C=C double bonds which provide some increased electrical conductivity through electrons. A completely decomposed or dehydrochlorinated form of PVC is polyacetylene, a conductive polymer.

3.5. Visual Observations

Figure 6 shows the color changes in both virgin and Al_2O_3 doped PVC with respect to aging time. As the amount of Al_2O_3 increases, and with increasing thermal aging time, the differences in color are pronounced. Increasing discoloration of PVC correlates very closely with the FTIR results that showed increased structural degradation through dehydrochlorination (the removal of hydrogen chloride), along with the formation of conjugated C=C bonds (the formation of conjugated double bonds) [39]. The chemical structural degradation process through the removal of hydrogen chloride to create the polyene chains (with conjugated C=C) is responsible for the observed discoloration.
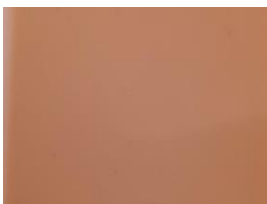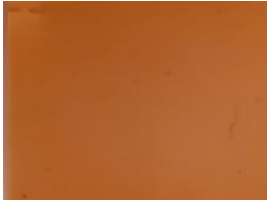
Aging	Al₂O₃ nanoparticles (wt%)			
Time (h)	0	2.5	5.0	7.5
0 h				
1200 h				
2400 h				

Figure 6. Thermal aging effects on the texture and coloration of virgin PVC and PVC/Al₂O₃ nanocomposites at different filler concentrations.

4. Conclusions

This study investigated the effect of thermal aging on PVC/Al₂O₃ nanocomposites. The samples were characterized using dielectric spectroscopy, charging/discharging current measurements, FTIR, SEM, and visual observations. All these properties were evaluated before and after thermal aging at 90 °C. The results indicate that the observed improvements in dielectric performance and resistance to aging, especially at carefully optimized filler concentrations, position PVC/Al₂O₃ nanocomposites as strong contenders for next-generation insulation in power transmission and distribution equipment, offering the potential for extended service life and enhanced operational reliability.

Based on the experimental results obtained from the characterization techniques, the key findings can be summarized as follows:

- The dielectric response of the PVC matrix was notably influenced by the Al₂O₃ nanofiller content. In unaged specimens, the permittivity exhibited increases of 6.9% and 3.6% at 2.5 wt% and 7.5 wt% loadings, respectively, highlighting a non-monotonic relationship between filler concentration and interfacial polarization.
- The inclusion of Al₂O₃ nanofillers measurably elevated the dielectric loss factor, with the 2.5 wt% and 7.5 wt% composites showing increases of 13% and 26%, respectively. These rises are consistent with the introduction of loss mechanisms like interfacial polarization, leading to greater energy dissipation.
- The initial electrical insulation characteristics were markedly enhanced by the nanofiller's incorporation. A clear trend of suppression in conduction currents was observed, with the steady-state charging current for the 7.5 wt% composite measuring 1.25×10^{-11} A, representing a 28% reduction from the 1.74×10^{-11} A value of the unfilled PVC.

The trapping efficiency was even more evident in the dissipation phase, where the discharging current decreased by 77%, falling from 2.52×10^{-12} A to 5.82×10^{-13} A.

- Prolonged thermal exposure induced a significant alteration of the electrical properties, culminating in a pronounced rise in conductivity. This is quantitatively demonstrated by the 7.5 wt% composite, whose charging current escalated to 1.70×10^{-11} A after 2400 h—a 36% increase from its initial state. The most dramatic change was witnessed in the depolarization current, which underwent an increase of over two orders of magnitude ($28\times$), reaching 1.66×10^{-11} A from an initial 5.82×10^{-13} A.
- FTIR and SEM analyses show that thermal aging induced the formation of some polar groups, likely due to structural decomposition and the small degree of dehydrochlorination.
- A significant color change was observed in the samples during the aging process, indicating surface degradation.

This study presents the first comprehensive investigation into the thermal aging behavior of PVC 4000 M reinforced with Al_2O_3 nanoparticles. The work demonstrates that these materials, fabricated using an industrially scalable calendering process, show complex electrical behavior during long-term thermal aging, accompanied by chemical changes including conjugated C=C bond formation and microstructural defects. Future work should utilize surface-modified nanoparticles to optimize interfacial adhesion and incorporate advanced characterization, such as thermogravimetric analysis/differential scanning calorimetry (TGA/DSC), energy-dispersive X-ray spectroscopy (EDX), and Brunauer–Emmett–Teller (BET). This will allow for the findings of this initial study to be interpreted within a comprehensive structure–property framework, enabling rational material design. While the study provides important insights into aging behavior, end-of-life recyclability remains an area for future investigation.

Author Contributions: Conceptualization, S.A. and A.H.; Methodology, A.D. and M.M.; Validation, S.R.; Formal analysis, A.M.H.; Investigation, D.C. All authors have read and agreed to the published version of the manuscript.

Data Availability Statement: The original contributions presented in this study are included in the article. Further inquiries can be directed to the corresponding authors.

Conflicts of Interest: The authors declare no conflict of interest.

References

1. Ibrahim, I.D.; Jamiru, T.; Sadiku, E.R.; Hamam, Y.; Alayli, Y.; Eze, A.A. Application of nanoparticles and composite materials for energy generation and storage. *IET Nanodielectr.* **2019**, *2*, 115–122. [CrossRef]

2. Rahman, M.M.; Khan, K.H.; Parvez, M.M.H.; Irizarry, N.; Uddin, M.N. Polymer Nanocomposites with Optimized Nanoparticle Dispersion and Enhanced Functionalities for Industrial Applications. *Processes* **2025**, *13*, 994. [CrossRef]

3. Hedir, A.; Lamrous, O.; Fofana, I.; Slimani, F.; Moudoud, M. Critical Issues in XLPE-Based Polymer Nanocomposites and Their Blends. *Mater. Horiz.* **2021**, *63*, 63–83.

4. Rahimi-Ahar, Z.; Rahimi-Ahar, L. Thermal, optical, mechanical, dielectric, and electrical properties of nanocomposites. *Eur. Polym. J.* **2024**, *218*, 113337. [CrossRef]

5. Fatemah, H.; Alkallas, A.; Al-Ahmadi, A.; Salem, E.; Mwafy, W.; Elsharkawy, W.; Trabelsi, A.B.G.; Motawea, M.; Alshammary, A.J.; Nafee, S.; et al. Influence of Al_2O_3 nanoparticles on the structural, optical, and electrical properties of PVC/PS nanocomposite for use in optoelectronic devices. *Surf. Interfaces* **2024**, *51*, 104651.

6. Elsad, R.A.; Habashy, M.M.; Izzularab, M.A.; Abd-Elhady, A.M. Evaluation of dielectric properties for PVC/SiO$_2$ nanocomposites under the effect of water absorption. *J. Mater. Sci. Mater. Electron.* **2023**, *34*, 786. [CrossRef]

7. Pagacz, J.; Chrzanowski, M.; Krucińska, I.; Pielichowski, K. Thermal aging and accelerated weathering of PVC/MMT nanocomposites: Structural and morphological studies. *J. Appl. Polym. Sci.* **2015**, *132*, 42090. [CrossRef]

8. He, L.; Ye, Z.; Zeng, J.; Yang, X.; Li, D.; Yang, X.; Chen, Y.; Huang, Y. Enhancement in electrical and thermal properties of LDPE with Al_2O_3 and h-BN as nanofiller. *Materials* **2022**, *15*, 2844. [CrossRef]

9. Sugumaran, C.P. Experimental study on dielectric and mechanical properties of PVC cable insulation with SiO_2/$CaCO_3$ nanofillers. In Proceedings of the 2015 IEEE Conference on Electrical Insulation and Dielectric Phenomena (CEIDP), Ann Arbor, MI, USA, 18–21 October 2015; pp. 503–506.

10. Nait Larbi, S.; Moudoud, M.; Hedir, A.; Lamrous, O.; Durmus, A.; Clark, D.; Slimani, F. Characterization of PVC/$CaCO_3$ nanocomposites aged under the combined effects of temperature and UV-radiation. *Materials* **2025**, *18*, 4001. [CrossRef]

11. Yaacob, M.M.; Kamaruddin, N.; Mazlan, N.A.; Noramat, N.F.; Alsaedi, M.A.; Aman, A. Dielectric Properties of Polyvinyl Chloride with Wollastonite Filler for the Application of High-Voltage Outdoor Insulation Material. *Arab. J. Sci. Eng.* **2014**, *39*, 3999–4012. [CrossRef]

12. Faiza; Khattak, A.; Alahmadi, A.A.; Ishida, H.; Ullah, N. Improved PVC/ZnO Nanocomposite Insulation for High Voltage and High Temperature Applications. *Sci. Rep.* **2023**, *13*, 7235. [CrossRef] [PubMed]

13. Xie, Y.; Liu, W.; Liang, L.; Liu, C.; He, S.; Zhang, F.; Shi, H.; Yang, M. Enhancement of anticorrosion property and hydrophobicity of modified epoxy coatings with fluorinated polyacrylate. *Colloids Surf. A Physicochem. Eng. Asp.* **2019**, *579*, 123659. [CrossRef]

14. Wang, Z.; Xie, T.; Ning, X.; Liu, Y.; Wang, J. Thermal degradation kinetics study of polyvinyl chloride (PVC) sheath for new and aged cables. *Waste Manag.* **2019**, *99*, 146–153. [CrossRef]

15. Bal, S.; Tamus, Z.A. Analyzing the impact of short-term cyclic thermal ageing on PVC insulated low voltage samples with polarization/depolarization current measurement. *Acta Polytech. Hung.* **2023**, *20*, 77–91. [CrossRef]

16. Nazrin, A.; Kuan, T.M.; Mansour, D.A.; Farade, R.A.; Mohd Ariffin, M.S.; Abd Rahman, N.I.B.A.W. Innovative approaches for augmenting dielectric properties in cross-linked polyethylene (XLPE): A review. *Heliyon* **2024**, *10*, e34737. [CrossRef]

17. Hamzah, M.S.; Mariatti, M.; Ismail, H. Melt flow index and flammability of alumina, zinc oxide and organoclay nanoparticles filled cross-linked polyethylene nanocomposites. *Mater. Today Proc.* **2019**, *17*, 798–802. [CrossRef]

18. Maur, S.; Haque, N.; Pottekat, P.; Chakraborty, B.; Dalai, S.; Chatterjee, B. Investigations on the effect of ageing on charge de-trapping processes of epoxy–alumina nanocomposites based on isothermal relaxation current measurements. *ET Nanodielectr.* **2020**, *3*, 116–123. [CrossRef]

19. Singha, S.; Thomas, M.J. Dielectric Properties of Epoxy-Al_2O_3 Nanocomposite System for Packaging Applications. *IEEE Trans. Compon. Packag. Technol.* **2010**, *33*, 373–385. [CrossRef]

20. Tang, Y.; Ge, G.; Li, Y.; Huang, L. Effect of Al_2O_3 with different nanostructures on the insulating properties of epoxy-based composites. *Materials* **2020**, *13*, 4235. [CrossRef]

21. Mansour, S.A.; Elsad, R.A.; Izzularab, M.A. Dielectric properties enhancement of PVC nanodielectrics based on synthesized ZnO nanoparticles. *J. Polym. Res.* **2016**, *23*, 85. [CrossRef]

22. Quader, R.; Narayanan, L.K.; Caldona, E.B. Dielectric characterization of fiber- and nanofiller-reinforced polymeric materials. *J. Appl. Polym. Sci.* **2024**, *141*, e55362. [CrossRef]

23. Habashy, M.M.; Abd-Elhady, A.M.; Elsad, R.A.; Izzularab, M.A. Performance of PVC/SiO_2 nanocomposites under thermal ageing. *Appl. Nanosci.* **2021**, *11*, 2143–2151. [CrossRef]

24. Jin, M.; Dong, M.; Ren, M.; Wu, X.; Shen, L.; Wang, H. Effect of nanoparticle polarization on relative permittivity of transformer oil-based nanofluids. *J. Appl. Phys.* **2013**, *113*, 204103. [CrossRef]

25. Zhang, T.; Zheng, Z.; Zhang, M.; Li, S.; Huang, H.; Zhang, Z. Investigation of dielectric properties and conductivity of polyvinyl chloride composites by terahertz time-domain spectroscopy. *Polym. Test.* **2024**, *134*, 108446. [CrossRef]

26. Amraoui, S.; Hedir, A.; Nait Larbi, S.; Moudoud, M.; Durmus, A. Evaluation of the electrical properties of XLPE cable insulation material aged under the combined effects of thermal stress and UV-radiation. In Proceedings of the 2024 3rd International Conference on Advanced Electrical Engineering (ICAEE), Sidi-Bel-Abbes, Algeria, 5–7 November 2024. [CrossRef]

27. Barber, P.; Balasubramanian, S.; Anguchamy, Y.; Gong, S.; Wibowo, A.; Gao, H.; Ploehn, H.J.; Zur Loye, H.-C. Polymer composite and nanocomposite dielectric materials for pulse power energy storage. *Materials* **2009**, *2*, 1697–1733. [CrossRef]

28. Gherasim, C.; Asandulesa, M.; Fifere, N.; Doroftei, F.; Tîmpu, D.; Airinei, A. Structural, optical and dielectric properties of some nanocomposites derived from copper oxide nanoparticles embedded in poly(vinylpyrrolidone) matrix. *Nanomaterials* **2024**, *14*, 759. [CrossRef]

29. You, L.; Liu, B.; Hua, H.; Jiang, H.; Yin, C.; Wen, F. Energy storage performance of polymer-based dielectric composites with two-dimensional fillers. *Nanomaterials* **2023**, *13*, 2842. [CrossRef]

30. Hedir, A.; Slimani, F.; Moudoud, M.; Bellabas, F.; Loucif, A. Impact of thermal constraint on the low-density polyethylene (LDPE) properties. *Lect. Notes Electr. Eng.* **2020**, *599*, 952–960.

31. Tan, D.Q. The search for enhanced dielectric strength of polymer-based dielectrics: A focused review on polymer nanocomposites. *J. Appl. Polym. Sci.* **2020**, *137*, 49379. [CrossRef]

32. Abdallah, H.; Sébastien, R.; Omar, J.; Ali, D.; Mustapha, M.; Omar, L.; Abderrahmane, M.H. Assessment of UV-aging of crosslinked polyethylene cable insulation by electrical measurements, FTIR and DSC analyses. *ECS J. Solid State Sci. Technol.* **2025**, *14*, 013008. [CrossRef]

33. Zhang, Y.Y.; Jiang, F.Y.; Yu, X.Y.; Zhou, K.; Zhang, W.; Fu, Q.; Hao, J. Assessment of thermal aging degree of 10kV cross-linked polyethylene cable based on depolarization current. *IEEE Access* **2021**, *9*, 111020–111029. [CrossRef]

34. Man, P.R.; Lin, Q.W.; Xu, J.; Wang, H.B.; Zhao, Y.H.; Su, W.W.; Lyu, H.F.; Li, Y. Thermal decomposition kinetics of poly(vinyl chloride) insulation for overloaded and non-overloaded wires. *J. Therm. Anal. Calorim.* **2025**, *150*, 11. [CrossRef]

35. Kotomin, E.A.; Stashans, A.; Kantorovich, L.N.; Lifshitz, A.I.; Popov, A.I.; Tale, I.A.; Calais, J.-L. Calculations of the geometry and optical properties of FMg centers and dimer (F2-type) centers in corundum crystals. *Phys. Rev. B* **1995**, *51*, 8770. [CrossRef]

36. Jacobs, P.W.M.; Kotomin, E.A.; Stashans, A.; Tale, I. Theoretical simulations of hole centres in corundum crystals. *Model. Simul. Mater. Sci. Eng.* **1994**, *2*, 109. [CrossRef]

37. Savchyn, V.P.; Popov, A.I.; Aksimentyeva, O.I.; Klym, H.; Horbenko, Y.Y.; Serga, V.; Moskina, A.; Karbovnyk, I. Cathodoluminescence characterization of polystyrene-BaZrO$_3$ hybrid composites. *Low Temp. Phys.* **2016**, *42*, 597–600. [CrossRef]

38. Starnes, W.H. Structural and Mechanistic Aspects of the Thermal Degradation of Poly(Vinyl Chloride). *Prog. Polym. Sci.* **2002**, *27*, 2133–2170. [CrossRef]

39. Benavides, R.; Castillo, B.M.; Castañeda, A.O.; López, G.M.; Arias, G. Different thermo-oxidative degradation routes in poly(vinyl chloride). *Polym. Degrad. Stab.* **2001**, *73*, 3. [CrossRef]

40. Starnes, W.H.; Ge, X. The Mechanism of Poly(Vinyl Chloride) Stabilization by Organotin Compounds. *J. Vinyl Addit. Technol.* **2004**, *10*, 116–121.